Egypt. J. Chem. Vol. 67, SI: M. R. Mahran, pp. **1093 - 1101** (2024)

Egyptian Journal of Chemistry

http://ejchem.journals.ekb.eg/

Synthesis and Characterization of hematoxylin biomolecule-doped polymeric nanocomposite film and evaluation of its performance as Low γ-ray Dosimeter applied to medical diagnosis

Yassine EL-Ghoul [1]*; Saleh Alashrah [2]; Chiraz Ammar [3].

[1] *Department of Chemistry, College of Science, Qassim University, Buraidah 51452, Saudi Arabia;*

[2] *Department of Physics, College of Science, Qassim University, Buraidah 51452, Saudi Arabia;*

[3] *Department of Fashion Design, College of Arts and Design, Qassim University, Buraidah 51452, Saudi Arabia;*

Abstract:

Currently, gamma dosimetry linked to public health is gaining more and more importance in the field of medical diagnosis. The use of different dyes, sensitive to radiation dose intensity, incorporated into different polymer biofilms has shown promising avenues for radiation dosimetry. Accordingly, the hematoxylin biomolecule as a low-ray dose sensitive dye will be integrated into a polyvinyl alcohol (PVA) polymeric host film. Direct detection of hematoxylin color change after irradiation with different γ-ray doses (2, 4, 10, and 20 mGy) was apparent allowing visual estimation of radiation dose. The impact of the different radiation exposures has been evaluated via FTIR, UV, optical, colorimetric, and SEM analysis. FTIR investigation revealed an obvious chemical change with increased doses. SEM investigation showed significant morphological alteration of PVA/HX films following radiation exposure. Moreover, the produced PVA/HX films displayed good pre- and post-irradiation stability in both dark and light conditions. Furthermore, response behaviors, deduced from the different characterizations, according to increasing γ-ray intensities have been recorded to assess their dosimetric potential for the routine γ-irradiation process. Indeed, the UV-Vis response curve demonstrated a linear rise in absorbance as radiation doses increased (R = 0.992). Similarly, the different varied parameters in the colorimetry study increased linearly with increasing γ-ray doses. The proposed novel dosimeter designed in nanoscale composite film might consequently offer an effective alternative for accurate and direct assessment of γ-ray low doses finding promising use in various medical applications.

Keywords: Hematoxylin; Polymer; PVA; nanocomposites; characterization; γ-ray dosimeter**;** irradiation; medical diagnostic radiology

1.INTRODUCTION

Radiation dosimetry has gained increasing attention in recent years. Its crucial objective was always, the accurate detection and precise control of different radiation treatments of materials and industrial products using electron beams and gamma rays [1,2].

The technique of radiation treatment is extensively applied in different fields involving routine dosimetry applications. These applied fields include Water remedy, food irradiation, polymerization, medical sterilization, and diagnostic radiology [3-7]. Different levels of radiation dose are investigated. the variation of the dose intensity classified as high, medium, or low specifies the field of application of the radiation. Currently, the accurate detection and assessment of the delivered radiation dose represent an essential requirement in many applications. The big challenge remains today with low doses given the unavailability of suitable dosimeters in this low range [8,9]. Different dosimetric solutions and alternatives for various dose levels were studied and reported recording rapid progress, including Geiger-Muller, photographic films, and proportional counter [10,11]. Furthermore, standard solutions as new dosimetric alternatives have appeared and their effectiveness has been widely evaluated. Their property of color and/or oxidation state change was at the origin of their high dosimetric performance [12,13]. However, these dosimetric solutions require severe conditions during their manipulation and their detection of change requires the presence of auxiliary instruments, in particular ESR, IR, NMR, UV-Vis, and thermoluminescence. These heavy instruments are usually expensive and impractical for easy and quick detection [14,15]. To address this challenge and achieve this goal, radiation-induced physical changes were the most effective approach. The key advantage is the ability to easily detect and even quantify the dose immediately upon analysis. As a result, this technique is based on the direct exploitation of the various changes resulting from the radiation dose.

Corresponding Author emaily.elghoul@qu.edu.sa* (Yassine EL-Ghoul,)

Receive Date: 02 October 2024, Revise Date: 30 October 2024, Accept Date: 12 November 2024

DOI: 10.21608/EJCHEM.2024.325402.10565

These changes could be physical, colorimetrical, and optical, which are easily detected on the designed dosimeter [16,17]. These changes in properties could be ensured by different dyeing molecules incorporated into different polymer matrices. The polymer solution casting method was the appropriate technique to prepare these nanocomposite films. Therefore, choosing a polymer that is easy to cast and able to interact with various host dyes while preserving their chemical and physical properties is fundamental for effective dosimeters [18,19]. Currently, functional polymers and polymer composites provide polymers with high added value and have proven their performance in many fields of application [20-24]. Different polymers have been studied as basic matrices of nanocomposite films applied in radiation dosimetry. Among these polymers are mainly polyamide, polyvinyl alcohol, polymethyl methacrylate, polystyrene, polyvinyl chloride, and cellulose acetate. These polymeric matrices have shown their efficiency to incorporate different classes of dyes and being effective as sensors for dosimetry devices [25-27]. The most widely used polymer via the casting method was PVA. The incorporation of different dye molecules into the PVA matrix has attracted great interest in several research studies [28,29]. The benefit of using PVA polymer as a matrix in the preparation of film dosimeters lies in its availability, low cost, biocompatibility, high water solubility, and ability as an environmentally friendly material to accommodate a large number of substrate hosts such as transition metals and dyes [30-32]. Different host coloring molecules were investigated in the PVA matrix to be applied as g-ray dosimeters. Indeed, Akhtar et al. have developed PVA films doped with a reactive dye methyl orange and they studied their dosimetric change after high irradiation processing [33]. AL Zahrany et al. have explored the methyl red dye as a sensing agent in PVA film studied as a radiochromic dosimeter. Results revealed the performance of the made film as a high-dose dosimeter up to 60 KGy [34]. Recently, Al-Hazmy et al. studied the performance of a new fluorescent dye based on boron difluoride complex (DBDMA) as an indicator after its incorporation in PVA film. Results showed its dosimetric efficiency after γ-irradiation exposure [35].

It is worth noting that the reported dosimeters were efficient against medium and high levels of gamma ray. Furthermore, most detecting molecules are synthetic dyes. The novelty and new aspect of this study is the use of hematoxylin as a natural and biocompatible substrate for a dosimeter sensitive to low doses of gamma radiation. Hematoxylin is a staining bioactive molecule widely applied in histology thanks to its sensitivity to color change. It is a natural product extracted from bloodwood trees, known for its excellent colorimetric and biological properties [36,37].

The current research study sought to create a highly sensitive, practical, cost-effective, and non-toxic gamma radiation dosimeter. Direct detection of hematoxylin color change after irradiation will allow visual estimation of radiation dose. After the optimization study of the parameters of synthesis of the nanocomposite thin film, the impact of the different radiation exposures will be evaluated via FTIR, UV, colorimetric, and SEM analysis. Furthermore, response behaviors, deduced from these characterizations, according to increasing γ-ray intensities were recorded in order to assess their dosimetric potential for the routine γ-irradiation process.

2. MATERIALS AND EXPERIMENTAL METHODS

2.1. Materials

The Hematoxylin natural product ($C_{16}H_{14}O_6$) used as matrix reinforcement for dosimetric doped films, and cellulose acetate polymer host (CA, MW= 95–114 kDa with a hydrolysis degree of 75–85%), were Sigma Aldrich products (St. Louis, USA). Their general structures are presented in Figure 1. For the synthesis of the different casted films, ultrapure water (Milli-Q® Direct, Darmstadt, Germany), was used as a solvent.

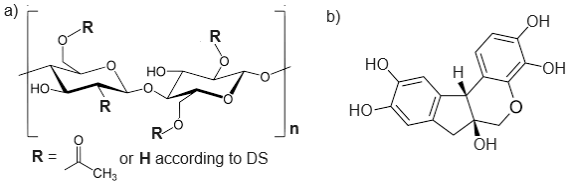

Figure 1. Chemical structures of a) the cellulose acetate and b) the hematoxylin biomolecule.

2.2. Characterization of Film Nanocomposites

Different techniques of characterization were performed to characterize the various casted nanocomposite films and to evaluate the impact of the g-ray exposures. Indeed, the detected chemical, physical colorimetric, and optical changes following increased radiation doses will be beneficial for the evaluation of the dosimetric performance of the designed films.

Chemical characterization via FTIR analysis using the attenuated total reflection (ATR) method was performed to record the various infrared spectra of raw and irradiated films. An infrared spectrophotometer apparatus (Agilent Technologies/Gladi-ATR, Santa Clara, CA, USA) was used. The different infrared spectra were recorded at a range of 4000 to 400 cm^{-1} and a resolution fixed at 4 cm^{-1}. UV absorption measurements of the different film labels were carried out using a UV–visible spectrophotometer (Shimadzu, UV-2501PC, Kyoto, Japan).

Wavelengths were varying in the range of 200 to 800 nm.

A Universal Testing Machine (Zwick Testing Machine Ltd., Leomister, UK) was used for the mechanical measurements. Samples were cut before tests in a rectangular form of 5 x 40 mm. Experiments were carried out under a fixed crosshead speed at 5 mm/min. Mechanical measurements were accomplished by evaluating the tensile strength of raw and irradiated samples following the standard ASTM D638. The temperature during tests was fixed at 22 °C with 65% of relative humidity. Five replicates were applied for each sample measurement and the averages were calculated.

The surface morphological evaluation of raw and irradiated film samples was performed via Scanning Electron Microscopy (SEM) analysis. A JEOL SEM device of JSM type-5400 LV (JEOL Ltd., Akishima, Japan). Measurements were carried out with an acceleration voltage of 5 kV and selected magnifications varied from 100 to 2000×. In the aim to obtain micrographs with good resolution, the surface conductivity of samples was improved by applying a thin layer coating of gold before analysis.

Colorimetric evaluation via the determination of the different color characteristics of raw and irradiated film samples was performed using a spectrocolorimeter (3-NH-YD 5010). The colorimetric device operates in the visible wavelength spectrum in the range varying from 380 to 780 nm. The following Kubelka–Munk equation 1 was used to determine the different color strength (K/S) values [38].

$$\frac{K}{S} = \frac{(1-R_\lambda)^2}{2\times R_\lambda} \quad (1)$$

K represents the absorption coefficient; S is the scattering factor and Rλ is the spectral reflectance of the film sample at λmax [39].

The different parameters L*, a*, and b* which represent the CIELab coordinates of the PVA/HX nanocomposite films were measured under a standard observer of 10° and the D65 as standard illuminant. The various ΔE values between raw and irradiated samples which represent the color total difference were deduced from these CIELab coordinates. L* is the lightness coordinate, a* and b* are the redness-greenness and the yellowness-blueness axis, respectively [40,41].

ΔE color total difference was calculated according to the following Equation 2.

$$\Delta E = \sqrt{(L*-L0)^2 + (a*-a0)^2 + (b*-b0)^2} \quad (2)$$

where (L*, a*, b*) and (L0, a0, b0) are the measured CIELab coordinates for the raw and irradiated PVA/HX film samples, respectively. The average limit of the distance ΔE between two CIELab coordinates is the value above which the human eye cannot differentiate. Many limits of ΔE depending mainly on color saturation have already been reported in various research works [42,43].

2.3. Preparation of PVA/HX Nanocomposite Films

PVA/HX casted films were synthesized according to the method reported previously by our research group [44]. Firstly, a bulk aqueous solution containing 5% PVA was prepared and heated at a constant temperature of 80 °C under vigorous stirring. two hours later, the solution became transparent and was cooled to ambient temperature. At this time a solution of hematoxylin was prepared by dissolving 0.02 g of HX in 10 mL of distilled water. The last prepared solution was then added to the viscous PVA solution and the mixture was stirred without heating to avoid the negative impact of heating on HX properties. After 30 min, each 20 ml of the prepared solution was transferred to glass petri dishes and kept to dry in the dark for 3 days at room temperature. Then the films were delicately peeled from the dishes and a thickness numerical instrument was used to determine their thickness measurements. Three separate measurements from different locations on the films are taken. The average film thickness was around 100 μm. The film labels were then stored at room temperature in dark black envelopes protected from light and UV rays to prevent their possible degradation and to reach the thermal equilibrium required for their subsequent application under adequate conditions.

3. Results and Discussion

3.1. Direct perception of color change after irradiation

The irradiation exposure of the different thin film labels exhibited a clear color change which is directly perceived with eyes. Results in Figure 2, show a gradual color deviation that increases with the dose of the γ-ray treatment. The exposed samples revealed a gradual degradation of color with the intensity of the g-ray dose from a purple to a dark reddish-brown shade. The change in color toward brown is due to the oxidization of the hematoxylin to hematein form [45]. This process is called ripening. These gradual deviations in shade detected after increased irradiation doses of very low intensity confirm the high sensitivity of these designed dosimetric films. Therefore, the PVA/HX films can be used as efficient dosimeters for the accurate control of the γ-ray exposure in diagnostic radiology.

3.2. Evaluation of the post-irradiation stability

The PVA/HX nanocomposite films treated with 20 mGy were kept in the light and dark under standard laboratory conditions (temperature 22 and 65% humidity) for 30 days. Using a UV spectrophotometer, the absorbance was determined at different storage periods at 575 nm. The results in Figure 3 showed no significant change in film stability over the testing period. Excellent stability was validated for films stored in light and dark,

throughout the 30-day storage period. These results were more effective than those of other dosimeters using other dopped polymeric casted films as gel or solution [46,47], which demonstrated poor stability, particularly when kept in the light. This could be related to the film-like casting which allows greater crystalline characteristics.

Figure 2. The color change in PVA/HX films after direct exposition to various γ-ray doses.

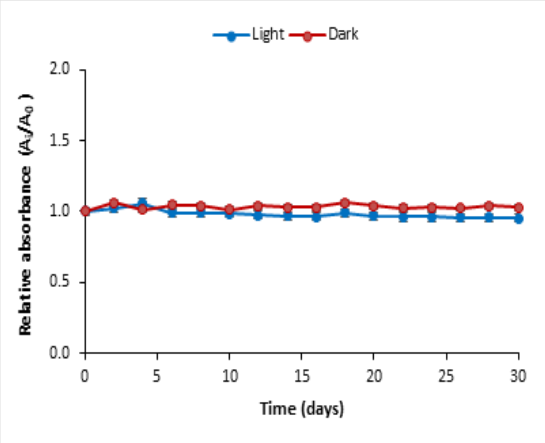

Figure 3. Study of the stability of the PVA/HX nanocomposite films at λmax of 430 nm, stored at room temperature in both light and dark conditions.

3.3. UV-visible absorption assessment

The UV-visible absorption study of the PVA/HX film, comprising 0.02 g of HX biomolecule, was carried out over the wavelength range of 200–700 nm. The spectra at different γ-ray doses are shown in Figure 4, where the absorption peak of the untreated film at 575 nm exhibited a gradual shift with increasing applied γ-ray dose.

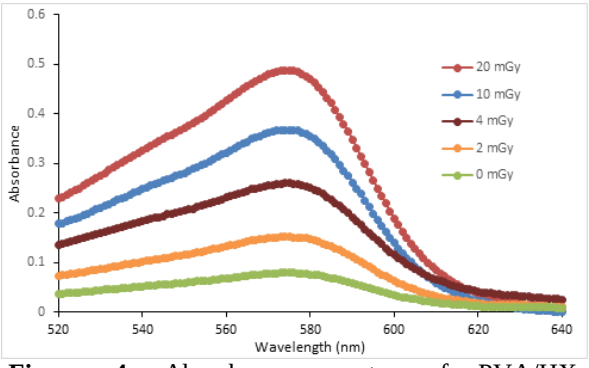

Figure 4. Absorbance spectra of PVA/HX nanocomposite films before and after exposition to varied γ-ray doses.

3.4. Response curve

The response curve of the nanocomposite PVA/HX films treated with various gamma-ray amounts is displayed in Figure 5. The response curves were created using the change in absorbance for each unit thickness, $\Delta A.mm^{-1}$, as a function of the dose received. At 575 nm, the absorbance values A0, and Ai for the unirradiated and irradiated films are represented by the formulas ΔA = A0 - Ai. With a significant coefficient of linear regression of R = 0.9826, the resulting curve displays a linear rise in absorbance according to increasing g-ray doses. This outcome is critical for the use of the PVA/HX produced films as very sensitive dosimeters, especially at extremely low radiation intensities.

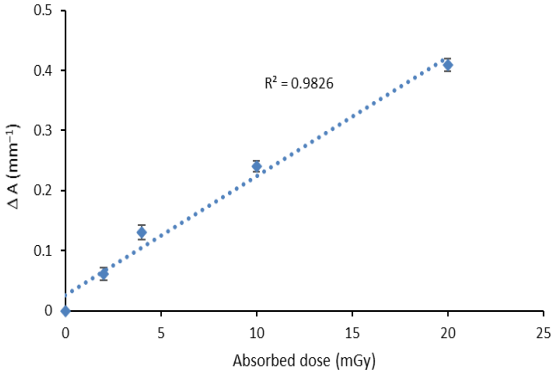

Figure 5 . Dose-response curve for PVA/HX films irradiated with different γ-ray doses according to the UV-Vis absorption capabilities at λmax

3.5. Infrared spectroscopy analysis

The effect of gamma rays on the structure of hematoxylin during increasing treatment times is first demonstrated by infrared spectroscopy (Figure 6). The modifications occurring, resulting from the oxidation process, are highlighted by the following FTIR spectra of the samples studied. Thus, the control sample of hematoxylin, which has both hydrogen bond donors and acceptors located to favor intramolecular hydrogen bonding, exhibits a slightly broadened O-H stretching absorption in the range of 3500 to 3600 cm^{-1}. In the case of treated hematoxylin, these bands decrease slightly with increasing γ-ray doses. This gradual decrease with increasing radiation levels is due to the oxidation of the hematoxylin to the hematein structure [45].

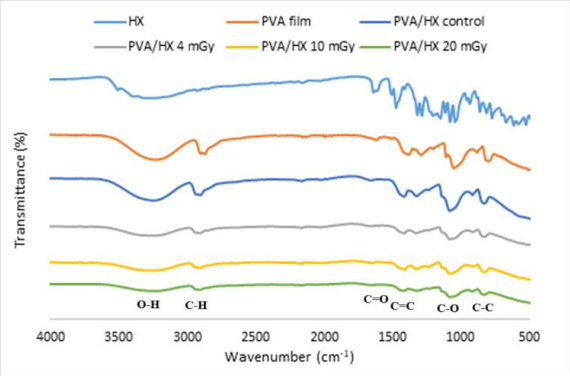

Figure 6. FTIR spectra of HX, PVA film, control PVA/HX film, and the different irradiated PVA/HX samples.

3.6. SEM morphology evaluation

SEM analysis was performed on untreated and irradiated PVA/HX films with increased γ-ray doses, to study their effects on surface morphology and microstructure. The PVA base film [48] and the untreated PVA/HX films are shown in Figure 7; these films have perfect structural integrity and are free of cracks. The good incorporation and dispersion of the guest molecule HX revealed a homogeneous film without solid phase separation thus allowing a smooth micro-appearance surface. The irradiated samples exhibited modified morphologies and the presence of aligned stripes on the surface. As the dose of g-rays applied increased, the obvious alterations in surface morphology intensified and the stripes became more pronounced and deeper. This implies that PVA/HX film is sensitive to low doses of γ-rays, making it an effective dosimeter for diagnostic purposes. This method has previously been used on PVA films with other synthetic guest molecules and gave comparable results before and after radiation exposure.

3.7. Spectrocolorimetric evaluation

For effective dosimeters, a directly perceptible change in color shade or intensity after radiation exposure is a crucial practical characteristic. To assess and measure the color deviation of PVA/HX films following their irradiation with various low γ-ray doses, a colorimetry investigation was carried out. Table 1 summarizes the average variation in CIELab parameter values L∗, a∗, b∗, K/S (color intensity), and ΔE (total color difference) for pristine and treated PVA/HX-produced films.

The variation of the CIELab color parameters according to the radiation dose exposed to the PVA/HX films is depicted in Figure 8. L* decreased with higher doses meaning that the films got darker. The color parameters a∗ and b∗ increased in absolute value with the dose intensity, this means that the tones of the films deviated towards more reddish and more bluish shades.

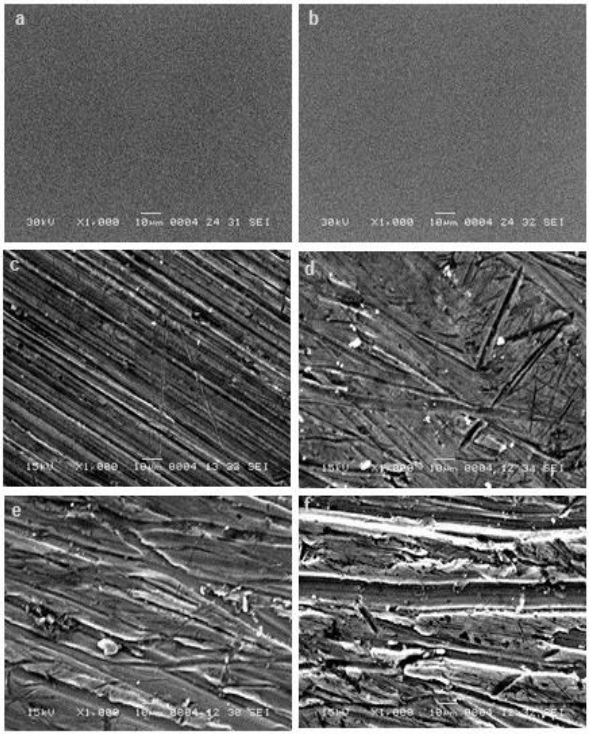

Figure 7. SEM micrographs of the nanocomposite films; (a) PVA film, (b) PVA/HX untreated film, (c) PVA/HX treated film with 2 mGy, (d) PVA/HX treated film with 4 mGy, PVA/HX treated film with 10 mGy, PVA/HX treated film with 20 mGy.

Table 1. Mean values of the CIELab parameters L∗, a∗, b∗, the ΔE and K/S values for untreated and g-irradiated PVA/HX films.

γ-ray dose	L*	a*	b*	ΔE	K/S
0	52.61	10.92	-3.32	-	5.45
4	54.1	11.25	-4.48	15.689	5.64
10	56.01	11.82	-6.27	17.920	5.91
20	58.96	12.61	-8.6	21.448	6.29

We observed a linear change with an excellent correlation of R= 0.99 for all these color coordinates. Due to their linear dependency with increased radiation dose, the color coordinate variables a*, b*, and L* can be explored separately as accurate dosimetry indices in the low dosage region of 0 to 20 mGy. Figure 8 shows that the total color difference ΔE levels increase as g-ray dosages are applied. We observed a linear change in determined ΔE with increased radiation exposures. Similarly, the color strength factor K/S grew with a linear manner with increasing g-ray exposure. Colorimetry analysis highlighted the significance of the created nanocomposite PVA/HX film as an accurate irradiation sensor and its prospective use as a new dosimetric system in the area of g-ray radiology for diagnostic purposes.

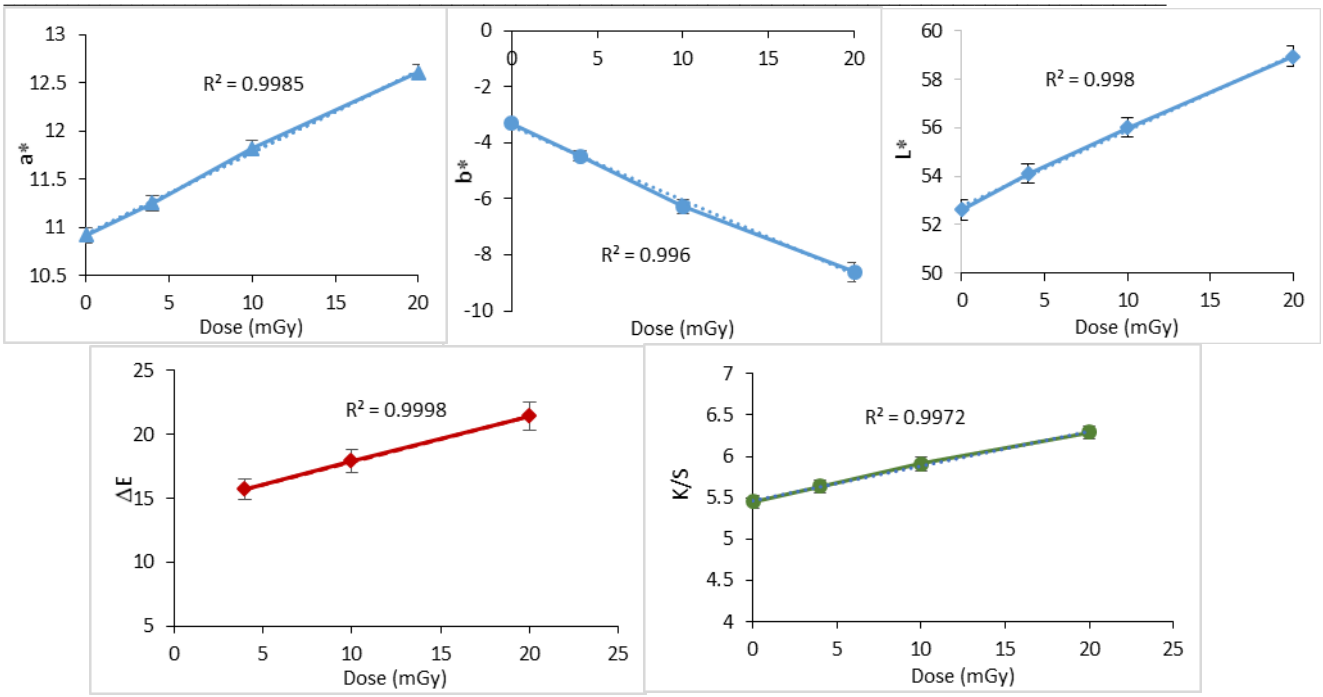

Figure 8. CIELab color parameters (L*, a* and b*), total color difference (ΔE), and color strength (K/S) values for PVA/HX films irradiated from 4 to 20 mGy.

Conclusion

Detecting or quantifying γ-ray doses to tissues or organs is crucial for risk prediction, but often difficult to detect directly. Thus, developing an efficient dosimetry method to handle low radiations in g-ray diagnostic radiography remains a significant challenge nowadays. In this study, we designed a new dosimetry system based on a PVA/HX nanocomposite film. Following exposure to progressively low doses of gamma radiation, the generated film demonstrated remarkable sensitivity in several chemical, physical, morphological, and colorimetric characterizations. Indeed, the results revealed a gradual rise in the absorption capability of the PVA/HX nanocomposite films as the applied dose increased. This was due to the oxidation of hematoxylin to the hematein structure caused by the g-rays irradiation. The resulting response curve determined by UV-visible absorptions demonstrated a linear rise in absorbance upon the increase of low-doses of γ-rays. The infrared chemical analysis validated the influence of applied radiations on the nanocomposite PVA/HX by revealing a gradual decrease in the OH band confirming thus the oxidation of the hematoxylin to the hematein structure with the augmentation in the irradiation level. SEM investigation revealed significant morphological alteration of PVA/HX films following irradiation, demonstrating their great sensitivity to very low gamma radiations. Furthermore, the produced PVA/HX films showed remarkable pre- and post-irradiation stability in both light and dark conditions for 2 to 30 days after exposure to low gamma radiation. The colorimetry study yielded the most significant findings since it indicated a clear observable change in color after increased irradiation exposure levels. This change in the color was quantified by calculating the different colorimetry parameters, the total color difference, and the color strength. All of these metrics increased linearly with the progressive augmentation of the γ-ray doses. These findings support the potential benefits of using PVA/HX thin films as highly sensitive dosimeters for routine medical diagnostic monitoring.

Funding: The authors gratefully acknowledge Qassim University, represented by the Deanship of Scientific Research, on the financial support for this research under the number 2023-SDG-1-BSRC36283 during the academic year 1445 AH / 2023 AD.

Institutional Review Board Statement: Not applicable.

Informed Consent Statement: Not applicable.

Conflicts of Interest: The authors declare no conflict of interest.

References

1. El-Kelany M, Gafar SM. Preparation of radiation monitoring labels to γ-ray. Optik, 2016. **127**: p. 6746-6753.
2. El-Ahdal MA, Gafar SM, Ebraheem S.A Colored Dosimeter Film for High Dose Applications. J Rad Res Appl Sci, 2011. **4**, No. 3(B): p. 855- 867.
3. Pati, S.; Chatterji, A.; Dash, B.P.; Raveen Nelson, B.; Sarkar, T.; Shahimi, S.; Atan Edinur, H.; Binti Abd Manan, T.S.; Jena, P.; Mohanta, Y.K.; et al. Structural

Characterization and Antioxidant Potential of Chitosan by γ-Irradiation from the Carapace of Horseshoe Crab. Polymers, 2020. **12**: p. 2361.

4. Hu, J.; Zhang, M.; He, Y.; Zhang, M.; Shen, R.; Zhang, Y.; Wang, M.; Wu, G. Fabrication and Potential Applications of Highly Durable Superhydrophobic Polyethylene Terephthalate Fabrics Produced by In-Situ Zinc Oxide (ZnO) Nanowires Deposition and Polydimethylsiloxane (PDMS) Packaging. Polymers, 2020. **12**: p. 2333.
5. Tapia-Guerrero, Y.S.; Del Prado-Audelo, M.L.; Borbolla-Jiménez, F.V.; Giraldo Gomez, D.M.; García-Aguirre, I.; Colín-Castro, C.A.; Morales-González, J.A.; Leyva-Gómez, G.; Magaña, J.J. Effect of UV and Gamma Irradiation Sterilization Processes in the Properties of Different Polymeric Nanoparticles for Biomedical Applications. Materials, 2020. **13**: p. 1090.
6. Peng, Y.K.; Lui, C.N.P.; Chen, Y.W.; Chou, S.W.; Raine, E.; Chou, P.T.; Yung, K.K.L.; Tsang, S.C.E. Engineering of Single Magnetic Particle Carrier for Living Brain Cell Imaging: A Tunable T1-/T2-/Dual-Modal Contrast Agent for Magnetic Resonance Imaging Application. *Chem. Mater*. 2017. **29**: p. 4411–4417.
7. Li, C.H.; Kuo, T.R.; Su, H.J.; Lai, W.Y.; Yang, P.C.; Chen, J.S.; Wang, D.Y.; Wu, Y.C.; Chen, C.C. Fluorescence-Guided Probes of Aptamer-Targeted Gold Nanoparticles with Computed Tomography Imaging Accesses for in Vivo Tumor Resection. *Sci. Rep.* 2015. **5**: p. 15675.
8. Inaba, Y.; Nakamura, M.; Zuguchi, M.; Chida, K. Development of Novel Real-Time Radiation Systems Using 4-Channel Sensors. Sensors, 2020. **20**: p. 2741.
9. Phong Vo, P.; Ngoc Doan, H.; Kinashi, K.; Sakai, W.; Tsutsumi, N.; Phu Huynh, D. X-ray Visualization and Quantification Using Fibrous Color Dosimeter Based on Leuco Dye. *Appl. Sci*. 2020. **10**: p. 3798.
10. Diffey, B. The Early Days of Personal Solar Ultraviolet Dosimetry. Atmosphere, 2020. ***11***: p. 125.
11. Kržanović, N.; Stanković, K.; Živanović, M.; Đaletić, M.; Ciraj-Bjelac, O. Development and testing of a low-cost radiation protection instrument based on an energy compensated Geiger-Müller tube. *Radiat. Phys. Chem.* 2019. **164**: p. 108358.
12. Glais, E.; Massuyeau, F.; Gautier, R. Tuning the oxidation states of dopants: A strategy for the modulation of material photoluminescence properties. *Chem. A Eur. J.* 2020. **27**(3): p. 905-914.
13. William, J.E. Tutorial on the Role of Cyclopentadienyl Ligands in the Discovery of Molecular Complexes of the Rare-Earth and Actinide Metals in New Oxidation States. Organometallics**,** 2016. **35**: p. 3088-3100.
14. Bhaskar, S.; Goswami, M.; Shobha, S.; Prakasan, V.; Krishnan, M.; Ghosh, S.K. Thermoluminescence and electron paramagnetic resonance study on rare earth/transition metal doped lithium borate glasses for dosimetry applications. *J. Lumin.* 2019. **216**: p. 116725.
15. Chandler, J.R.; Sholom, S.; McKeever, S.W.S.; Hall, H.L. Thermoluminescence and phototransferred thermoluminescence dosimetry on mobile phone protective touchscreen glass. *J. Appl. Phys.* 2019. **126**: p. 074901.
16. Vo, P.P.; Doan, H.N.; Kinashi, K.; Sakai, W.; Tsutsumi, N. X-ray composite fibrous color dosimeter based on 10,12-pentacosadiynoic acid. Dyes Pigments, 2021. **191**: p. 109356.
17. AL Zahrany, A.; Rabaeh, K.; Eyadeh, M.; Basfar, A. Dosimetric evaluation of methyl red radiochromic film for radiation processing. Pigment and Resin Technology, 2020. **50**: p. 157-162.
18. Ozkan Loch, C.; Eichenberger, M.A.; Togno, M.; Zinsli, S.P.; Egloff, M.; Papa, A.; Ischebeck, R.; Lomax, A.J.; Peier, P.; Safai, S. Characterization of a Low-Cost Plastic Fiber Array Detector for Proton Beam Dosimetry. Sensors, 2020. **20**: p. 5727.
19. Santos, T.; Ventura, T.; Lopes, M.d.C. A review on radiochromic film dosimetry for dose verification in high energy photon beams. *Radiat. Phys. Chem*. 2020. **179**: p. 109217.
20. Alminderej, F.M.; Ammar, C.; El-Ghoul, Y. Functionalization, characterization and microbiological performance of new biocompatible cellulosic dressing grafted chitosan and Suaeda fruticosa polysaccharide extract. Cellulose, 2021. **28**: p. 9821-9835.
21. EL-Ghoul, Y.; Ammar, C.; Alminderej, F.M.; Shafiquzzaman, M. Design and Evaluation of a New Natural Multi-Layered Biopolymeric Adsorbent System-Based Chitosan/Cellulosic Nonwoven Material for the Biosorption of Industrial Textile Effluents. Polymers, 2021. **13**: p. 322.
22. Ammar, C.; Alminderej, F.M.; EL-Ghoul, Y.; Jabli, M.; Shafiquzzaman, M. Preparation and Characterization of a New Polymeric Multi-Layered Material Based K-Carrageenan and Alginate for Efficient Bio-Sorption of Methylene Blue Dye. Polymers, 2021. **13**: p. 411.
23. El-Ghoul, Y. Biological and microbiological performance of new polymer-based chitosan

and synthesized aminocyclodextrin finished polypropylene abdominal wall prosthesis biomaterial. *Text. Res. J.* 2020. **90**: p. 2690–2702.
24. El-Ghoul, Y. and Alminderej, F.M. Bioactive and superabsorbent cellulosic dressing grafted alginate and Carthamus tinctorius polysaccharide extract for the treatment of chronic wounds. Textile Research Journal, 2021. **91**(3-4): p. 235-248.
25. Sąsiadek, E.; Jaszczak, M.; Skwarek, J.; Kozicki, M. NBT-Pluronic F-127 Hydrogels Printed on Flat Textiles as UV Radiation Sensors. Materials, 2021. **14**: p. 3435.
26. Seito, H.; Ichikawa, T.; Hanaya, H.; Sato, Y.; Kaneko, H.; Haruyama, Y.; Watanabe, H.; Kojima, T. Application of clear polymethylmethacrylate dosimeter Radix W to a few MeV electron in radiation processing. *Radiat. Phys. Chem.* 2009. **78**: p. 961–965.
27. Rabaeh, K.A.; Basfar, A.A. A polystyrene film dosimeter containing dithizone dye for high dose applications of gamma-ray source. *Radiat. Phys. Chem.* 2020. **170**: p. 108646.
28. Doyan, A.; Susilawati, S.; Prayogi, S.; Bilad, M.R.; Arif, M.F.; Ismail, N.M. Polymer Film Blend of Polyvinyl Alcohol, Trichloroethylene and Cresol Red for Gamma Radiation Dosimetry. Polymers, 2021. **13**: p. 1866.
29. Susilawati, S.; Prayogi, S.; Arif, M.F.; Ismail, N.M.; Bilad, M.R.; Asy'ari, M. Optical Properties and Conductivity of PVA–H3PO4 (Polyvinyl Alcohol–Phosphoric Acid) Film Blend Irradiated by γ-Rays. Polymers, 2021. **13**: p. 1065.
30. Osman, M.I.; Abdalla, D.M.; Elfaki, H.A.; Yagoub, Y.A.K.; Ibrahim Hussein, K.; Eldoma, M.A.; Omer Al-atta, N.; Mohamed Osman Siddig, Y. Effects of additive and gamma irradiation on the structural and optical properties of polyvinyl alcohol doped with silver nitrate. *Glob. Sci. J.* 2021. **9**: p. 1780–1792.
31. Raouafi, A.; Daoudi, M.; Jouini, K.; Charradi, K.; Hamzaoui, A.H.; Blaise, P.; Farah, K.; Hosni, F. Effect of gamma irradiation on the color, structure and morphology of nickel-doped polyvinyl alcohol films: Alternative use as dosimeter or irradiation indicator. *Nucl. Instrum. Methods Phys. Res. Sect. B Beam Interact. Mater. At.* 2018. **425**: p. 4–10.
32. Alashrah, S.; El-Ghoul, Y.; Omer, M.A.A. Synthesis and Characterization of a New Nanocomposite Film Based on Polyvinyl Alcohol Polymer and Nitro Blue Tetrazolium Dye as a Low Radiation Dosimeter in Medical Diagnostics Application. Polymers, 2021. **13**: p. 1815.
33. Akhtar, S.; Hussain, T.; Shahzad, A.; Ul-Islam, Q.; Hussain, M.Y.; Akhtar, N. Radiation Induced Decoloration of Reactive Dye in PVA Films for Film Dosimetry. Journal of Basic & Applied Sciences, 2021. **9**: p. 416–419.
34. AL Zahrany, A., Rabaeh, K., Eyadeh, M. and Basfar, A. Dosimetric evaluation of methyl red radiochromic film for radiation processing. *Pigment & Resin Technology*, 2021. **50** (2): p. 157-162.
35. Al-Hazmy, S.M., El-Ghoul, Y., Al-Harby, J., Tar, H. and Alminderej, F.M. Synthesis, Characterization, and Performance of Pyridomethene–BF2 Fluorescence Dye-Doped PVA Thin Film and PVP Nanofibers as Low γ-ray Dosimeters. *ACS omega*, 2022. **7**(38): p. 34002-34011.
36. Ortiz-Hidalgo, C. and Pina-Oviedo, S. Hematoxylin: Mesoamerica's gift to histopathology. Palo de Campeche (logwood tree), pirates' most desired treasure, and irreplaceable tissue stain. International Journal of Surgical Pathology, 2019. **27**(1): p. 4-14.
37. Alminderej, F.M. and El-Ghoul, Y. Synthesis and study of a new biopolymer-based chitosan/hematoxylin grafted to cotton wound dressings. Journal of Applied Polymer Science, 2019. **136**(23): p. 47625.
38. Lee, H. C. Introduction to color imaging science. New York, NY: Cambridge University Press. 2005.
39. Kuehni, R.G. Color: An introduction to practice and principles (2nd ed.). Hoboken, NJ: John Wiley. 2005.
40. Schanda, J. Colorimetry: Understanding the CIE system. Hoboken, New Jersey, John Wiley. 2007.
41. Shams-Nateri, A. Effect of a standard colorimetric observer on the reconstruction of reflectance spectra of colored fabrics. Coloration Technology, 2008. **124**: p. 14–18.
42. McGrath, J.R.; Beck, M.; Hill, M.E. Replicating Red: Analysis of ceramic slip color with CIELAB color data. Journal of Archaeological Science: Reports, 2017. **14**: p. 432-438.
43. Johnston, W.M.; Kao, E. C. Assessment of Appearance Match by Visual Observation and Clinical Colorimetry. Journal of Dental Research, 1989. **68**(5): p. 819-822.
44. Alashrah, S.; El-Ghoul, Y.; Almutairi, F.M.; Omer, M.A.A. Development, Characterization and Valuable Use of Novel Dosimeter Film Based on PVA Polymer Doped Nitro Blue Tetrazolium Dye and

AgNO3 for the Accurate Detection of Low X-ray Doses. Polymers, 2021. **13**: p. 3140.

45. Chiriac, A.P., Nita, L.E., Neamtu, I., Popescu, C.M., Ioanid, A. and Ioanid, G.E., 2005. Hematoxylin plasma treatment. Romanian Journal of Physics, **50**(9/10): p.1119.
46. El Gohary, M.I.; Soliman, Y.S.; Amin, E.A.; Gawad, M.H. A.; Desouky, O.S. Effect of perchloric acid on the performance of the Fricke xylenol gel dosimeter. Applied Radiation and Isotopes, 2016. **113**: p. 66-69.
47. Abdel-Fattah, A.A.; Beshir, W.B.; Hassan, H.M.; Soliman, Y.S. Radiation-induced coloration of nitro blue tetrazolium gel dosimeter for low dose applications. Radiation Measurements, 2017. **100**: p. 18-26.
48. Chen, S.A.; Fang, W.G. Electrically conductive polyaniline-poly(vinyl alcohol) composite films: physical properties and morphological structures. Macromolecules, 1991. **24**(6): p. 1242-1248.